

Classic PIV and Stereo-PIV Techniques in the Analysis of Turbulent Flow in a Stirred Tank

Aline G. De Mitri¹, Rodrigo de L. Amaral², Jenniffer S. Ayala¹, Helder L. de Moura³,
Guilherme J. de Castilho¹

¹Process Engineering Department, School of Chemical Engineering, University of Campinas
Albert Einstein Ave., 500 – Zip Code: 13083-852, Campinas-SP, Brazil
a093335@dac.unicamp.br; j192526@dac.unicamp.br; guijcas@unicamp.br

²Department of Mechanical Engineering, POLI, University of São Paulo
Prof. Luciano Gualberto Ave., 380 – Zip Code: 05508-030, São Paulo-SP, Brazil
rodrigoamaral@usp.br

³Center for Petroleum Studies, University of Campinas
Cora Coralina St., 350 – Zip Code: 13083-896, Campinas-SP, Brazil
helderlima@feq.unicamp.br

Abstract - Stirred tanks with multiphase mixtures in turbulent flow have numerous applications in industry. In this regime, the dispersed phase introduces flow structures at different scales from those observed in a single-phase system, thus impacting the moment, energy and mass transfer phenomena within the equipment. In this context, the proper measurement of turbulent parameters becomes crucial for better understanding the flow and developing more accurate models. One way to assess the fluid dynamics in this system is the application of imaging techniques, such as Particle Image Velocimetry (PIV). In its classic configuration (PIV), one camera evaluates a two-dimensional plane and obtains two velocity components (radial and axial). In its stereoscopic arrangement (Stereo-PIV), two cameras are positioned to assess the same two-dimensional plane, but they allow the reconstruction of the third velocity component (tangential). This work aims to investigate the application of these techniques to analyze the flow and turbulent kinetic energy (TKE) distribution in a tank stirred by a 45° pitched blade turbine (PBT). Three main criteria are considered: the experimental technique (PIV with two camera position settings and Stereo-PIV); the image plane, regarding the impeller blade angles of 0° and 45°; and the pseudo-isotropic assumption for TKE estimation. The results indicated that the best procedure for measuring turbulent parameters depends on all three criteria combined. In the case of the flow promoted by the PBT impeller, the PIV with the less tilted camera presented similar results to the Stereo-PIV using a simpler and more economical setup in terms of computational and experimental costs. The pseudo-isotropic assumption proved to be less suitable in the case of classic PIV with a greater camera tilt. In this case, due to the perspective error, the radial component seems to be overestimated, leading to higher estimates for TKE.

Keywords: stirred tank, particle image velocimetry, pitched blade impeller, pseudo-isotropic assumption, flow pattern.

1. Introduction

Stirred tanks are widely used in the most diverse industrial processes and often involve mixing components in multiphase systems, such as gas dispersions, emulsions formation and mixtures of solids and liquids. The combination of phases leads to changes in the flow dynamics and the balance between inertial and viscous forces [1]. In a turbulent regime, the dispersed phase introduces flow structures at different scales from those observed in a single-phase system, impacting the moment, energy and mass transfer phenomena developed within the equipment [2]. These structures make the measurements of turbulent parameters quite challenging. At the same time, obtaining this information is significant as operations design and optimization still depend on holistic rules or trial and error type experiments.

Particle Image Velocimetry (PIV) is a common non-intrusive technique applied to assess the flow in stirred tanks. Its operation is based on evaluating light scattering images caused by tracer particles and recorded in high-speed cameras. The acquisition of particle images at two different moments allows the determination of the flow field [3]. Other measurement systems can be considered when particle image velocimetry is applied. Among them, the classic PIV stands out, in which two velocity components are obtained from a two-dimensional plane. Similarly, the Stereoscopic PIV (Stereo-PIV) has

been widely applied. In this configuration, two cameras are used in an angular arrangement to obtain three velocity components in the same two-dimensional plane.

One way to analyze the distribution of turbulent kinetic energy (TKE) is through the evaluation of velocity fluctuations in a cross-section of the flow [4]. A widely used hypothesis in the literature for this estimate is the pseudo-isotropic flow assumption, which considers that the velocity components are independent of the measurement direction so that the tangential component can be computed as the arithmetic mean of the two measured velocities. The main problem with this assumption in the analysis of turbulent flow from stirred tanks is that the drag vortices generated by the impeller have a clearly defined orientation, making the approximation not very consistent with the reality of the phenomenon [5]. The Stereo-PIV technique can be considered a way to solve the issue of the lack of measurements of the tangential velocity component and the inconsistency of the pseudo-isotropic assumption in the acquisition of turbulent regime data [4]. However, it is a system that requires greater control over noise and may present difficulties in terms of the necessary optical access, in addition to higher costs related to the experimental apparatus, processing and data storage.

This work aims to investigate the best configuration of particle image velocimetry technique for analyzing the flow and turbulent kinetic energy distribution of a tank agitated by a 45° pitched blade turbine (PBT). The investigation considered three main criteria: the experimental technique (PIV with two camera position settings and Stereo-PIV); the plane of analysis regarding the angles in relation to the impeller blade (0° and 45°); and the pseudo-isotropic condition on the TKE estimation.

2. Experimental Setup

The system used in this study consisted of a cylindrical acrylic tank with a standard ASME torispherical bottom equipped with a 45° pitched blade turbine (PBT) with four blades angled at 45° and four metallic baffles equally spaced. The vessel diameter was $T = 0.38$ m, the impeller diameter $T/3$ and the baffle width $T/12$. The turbine was positioned at a clearance of $T/3$. The impeller rotational speed used was 660 rpm (11 rev/s) and the experiments were carried out with water as the working fluid (density $\rho = 998.2$ kg/m³ and viscosity $\mu = 1.003 \times 10^{-3}$ Pa·s) in a turbulent flow regime with Reynolds number of 1.76×10^5 . The liquid height was equal to the tank diameter ($H = T$).

The data acquisition was carried out using the experimental setup described in Figure 1 and it is composed of two identical *FlowSense EO 8M-21* cameras (3312 x 2488 pixels, 5Hz) and one *Nd:YAG* laser (532 nm, 200 mJ), which generated a light sheet with 2 mm thickness. The lens axes of both cameras were arranged so that Camera 1 was placed at an angle of $\sigma + \beta = 40^\circ$ relative to the normal vector of the object plane and Camera 2 was set at $\sigma = 10^\circ$. Despite the non-usual configuration, the *Scheinmpflug* principle was respected [6]. These positions were selected to decrease the image distortion caused by the curvature of the tank. Silver-coated glass spheres ($d_p = 10$ μm) were used as tracer particles. Angle-resolved (AR) measurements were made at two fixed blade positions, AR 0° and AR 45°. An encoder enabled the synchronization between the laser pulse, impeller movement and the camera trigger. For each blade position, 1000 pairs of images were recorded in both cameras in double-frame mode with an interframe time of 100 μs.

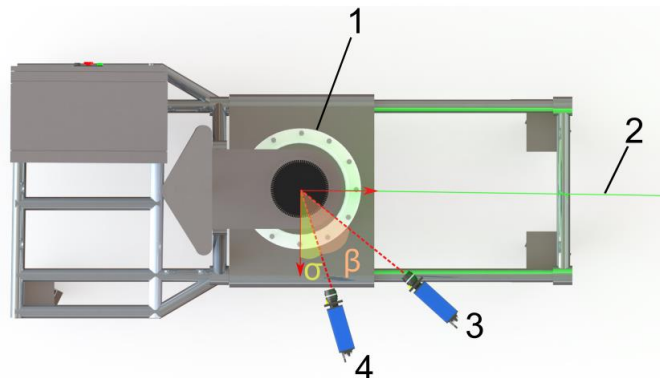


Fig. 1: Experimental setup with 1. Mixing system, 2. Laser sheet light, 3. Camera 1 and 4. Camera 2 (Adapted from [7])

The system was calibrated based on the method developed by Soloff et al. [8] for distortion compensation through a third-order polynomial function. A polymer plate was used as a target, containing 0.5 mm diameter points equally spaced by 1.5 mm. The cameras obtained the target images in the positions described in Figure 1. The data acquisition and calibration were performed by *Dantec Dynamic Studio* software. After the image acquisition, PIV and Stereo-PIV measurements were computed considering three distinct stages: pre-processing, processing and post-processing. In pre-processing, filters (Gaussian, subtraction by local minimum and intensity capping) were applied to optimize particle image format and eliminate background noise with MATLAB (MathWorks Inc, version 2018a) software. In the processing stage, standard cross-correlation (SCC) was implemented and optimized by an iterative multigrid strategy with variations of the interrogation window [9], [10]. In this strategy, the processing was made in four steps. In each step, the interrogation window size was progressively reduced with a percentage of overlap between the neighboring windows. The four steps considered interrogation windows with 64 x 64 pixels, 48 x 48 pixels, 32 x 32 pixels and 24 x 24 pixels, respectively. The overlap between interrogation windows was 25%, resulting in a final area of 18 x 18 pixels. This stage was performed using the PRANA toolbox [11] with MATLAB. After each step, simple post-processing based on the work of Westerweel and Scarano [12] was performed to eliminate outliers. In addition, complete post-processing considering the mean absolute deviation method (MAD) was applied based on the method developed by Barbutti et al. [13].

2.1. Turbulent Kinect Energy

The turbulent kinetic energy (k_{3C}) for the Stereo-PIV measurements was estimated from Eq. (1):

$$k_{3C} = \frac{1}{2} \left(\overline{u'^2} + \overline{v'^2} + \overline{w'^2} \right) \quad (1)$$

where $\overline{u'^2}$, $\overline{v'^2}$ e $\overline{w'^2}$ are the root mean square velocities in radial, axial and tangential directions, respectively. These components are calculated according to Eq. (2) for the radial direction, for example (the other directions follow the same model):

$$\overline{u'^2} = \overline{(u - \bar{u})^2} \quad (2)$$

where u and \bar{u} are instantaneous and time-averaged axial velocities, respectively. Two different assumptions were made for PIV measurements, in which the third velocity component (in the z direction) is not known. First, it is assumed that this component is pseudo-isotropic, then the turbulent kinetic energy is calculated according to Eq. (3):

$$k_{iso} = \frac{1}{2} \left[\overline{u'^2} + \overline{v'^2} + \frac{1}{2} \left(\overline{u'^2} + \overline{v'^2} \right) \right] = \frac{3}{4} \left(\overline{u'^2} + \overline{v'^2} \right) \quad (3)$$

Second, it is assumed that the flow is non-isotropic and the out-of-plane component is zero on the image plane of analysis; therefore, the turbulent kinetic energy is estimated by the Eq. (4):

$$k_{2C} = \frac{1}{2} \left(\overline{u'^2} + \overline{v'^2} \right) \quad (4)$$

3. Results and Discussion

3.1 Time-Averaged Velocity Fields

Fig. 2 and 3 show the time-averaged velocity fields of the radial (\bar{u}) and axial (\bar{v}) components, respectively, measured by (a) PIV-Camera 1, (b) PIV-Camera 2 and (c) Stereo-PIV for the blade angles AR 0° and AR 45° . Fig. 4 presents the time-averaged velocity fields of the tangential component obtained by the Stereo-PIV method. All the components were normalized by U_{tip} (impeller tip velocity, $U_{tip} = \pi DN \cong 4.33 \text{ m/s}$). Regardless of the impeller position, it can be verified that the radial component fields (Fig. 2) obtained by the PIV-Camera 1 have higher values than those obtained by the PIV-Camera 2 and Stereo-PIV fields. In fact, the maximum value for AR 0° was $0.54U_{tip}$ in the first case, while the other techniques presented a maximum of $0.42U_{tip}$ for the same blade position. In the case of AR 45° , the maximum \bar{u} value for PIV-Camera 1 was $0.55U_{tip}$, while PIV-Camera 2 and Stereo-PIV identified the highest values as $0.34U_{tip}$ and $0.40U_{tip}$, respectively. However, the axial component fields (Fig. 3) obtained by all techniques presented similar values, with an absolute maximum of $0.62U_{tip}$ for all approaches. The higher value of the radial component for the PIV - Camera 1 technique can be associated with the perspective error due to the more tilted positioning of the camera so that this component has its values overestimated and influenced by the tangential component (out-of-plane velocity).

The flow presented a strongly downward axial pattern due to the movement induced by the down-pumping pitched-blade turbine. As a result, the axial velocity component predominates in the flow, influenced by the radial and tangential components in the discharge zone below the impeller. In this region, more expressive values of the radial and tangential components were observed, which can be attributed to the blade movement. The comparison between the angle-resolved measurements allows verifying that the highest absolute values of the velocity components followed trailing vortices induced by the impeller. It can be observed the movement of the vortices from the suction region at AR 0° to the discharge region at AR 45° , which presented a slight deviation due to the pitched blade. The velocity components fields agreed with the results of Khan et al. [14], who observed the trailing vortices detachment between AR 0° and AR 45° when analyzing the flow promoted by the same type of impeller used in this work.

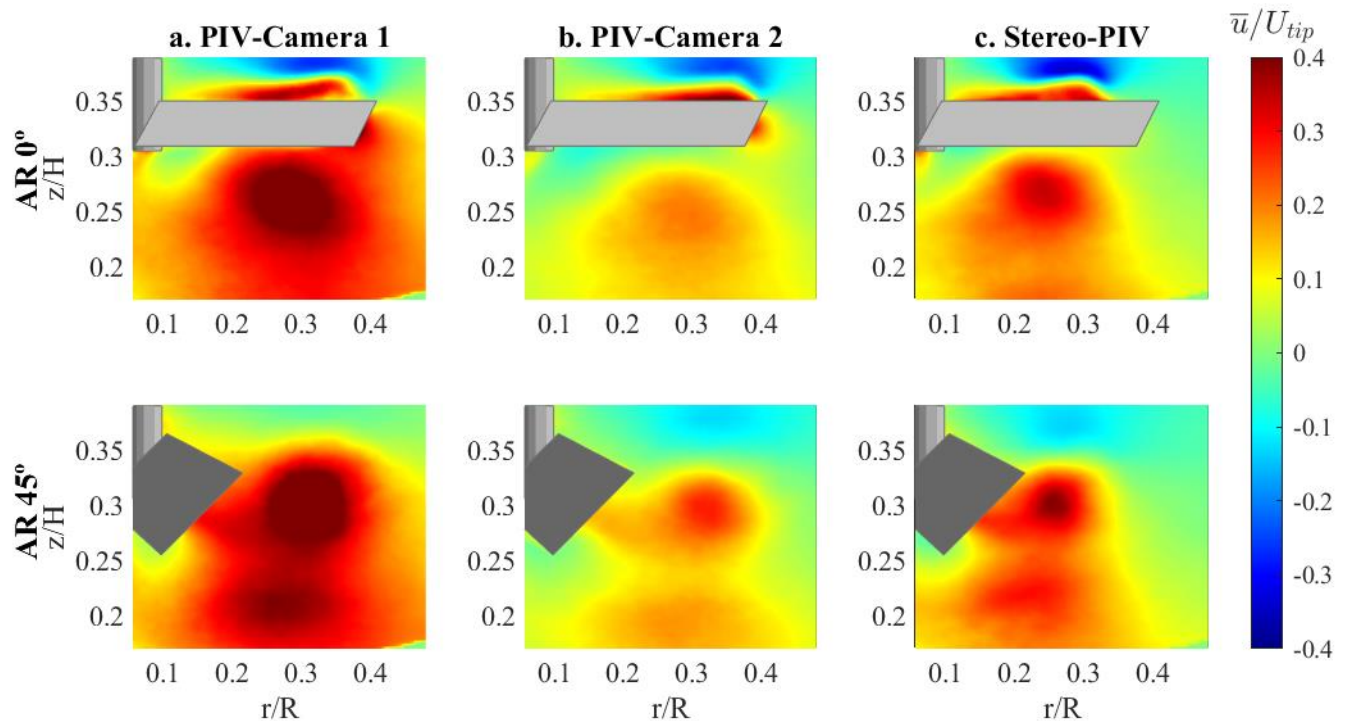


Fig. 2: Time-averaged radial component velocity (\bar{u}) fields considering (a) PIV-Camera 1, (b) PIV-Camera 2 and (c) Stereo-PIV at AR 0° and AR 45° .

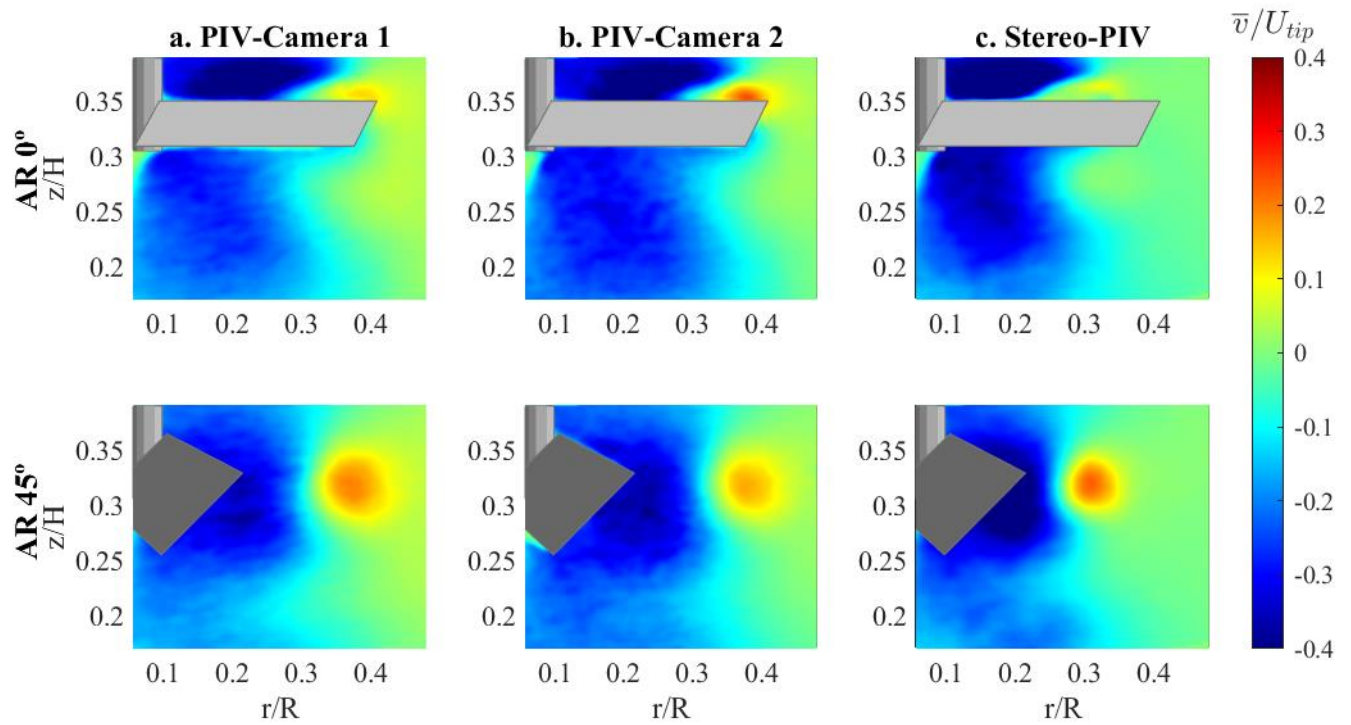


Fig. 3: Time-averaged axial component velocity (\bar{v}) fields considering (a) PIV-Camera 1, (b) PIV-Camera 2 and (c) Stereo-PIV at AR 0° and AR 45° .

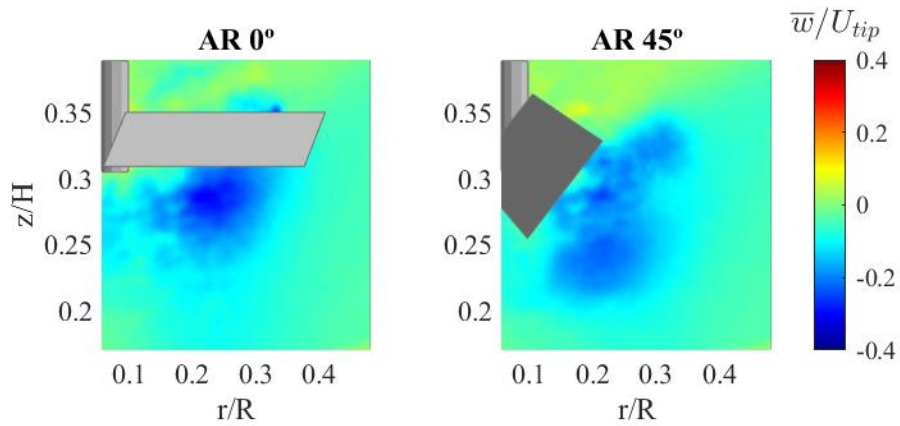


Fig. 4: Time-averaged tangential component velocity (\bar{w}) fields measured by Stereo-PIV at AR 0° and AR 45° .

3.2 Turbulent Kinetic Energy Fields

Fig. 5 and 6 show the turbulent kinetic energy fields estimated by PIV-Camera 1 and PIV-Camera 2, respectively, considering (a) the pseudo-isotropic assumption and (b) the non-isotropic approximation. Fig. 7 presents the TKE fields computed by Stereo-PIV measurements, taking all three velocity components into account. In all cases, the parameters were normalized by the square of the tip velocity (U_{tip}^2). The three techniques showed that the turbulent kinetic energy is concentrated in the region of the trailing vortices formation and followed its movement from the suction region (above the turbine), at AR 0°, to the discharge region (below the turbine), at AR 45°. However, because of the differences observed on the radial velocity component measurement, the TKE fields for the PIV-Camera 1 technique display higher values on the trailing vortices region, especially when the pseudo-isotropic assumption is considered and at AR 45°. In this situation, the maximum value for TKE was $0.11U_{tip}^2$ (at $r/R = 0.27$ and $z/H = 0.33$) for PIV-Camera 1 (Fig. 5a), while for PIV-Camera 2, the higher value was $0.09U_{tip}^2$, at the same region, as shown in Fig. 6a.

The comparison among the different approaches on the TKE estimation by PIV-Camera 2 and Stereo-PIV has shown that the pseudo-isotropic assumption tends to overestimate the TKE values (Fig. 6a). At the same time, the non-isotropic approximation (Fig. 6b) led to similar results with those obtained by the Stereo-PIV method, which considers all three velocity components (Fig. 7). This result can suggest that the PIV-Camera 2 technique is the more suitable arrangement because it shows similar information related to the Stereo-PIV setup. The classic PIV system is simpler, more economical, needs only one acquisition equipment, has better optical access and reduces the demand for noise control, processing and storage capacity.

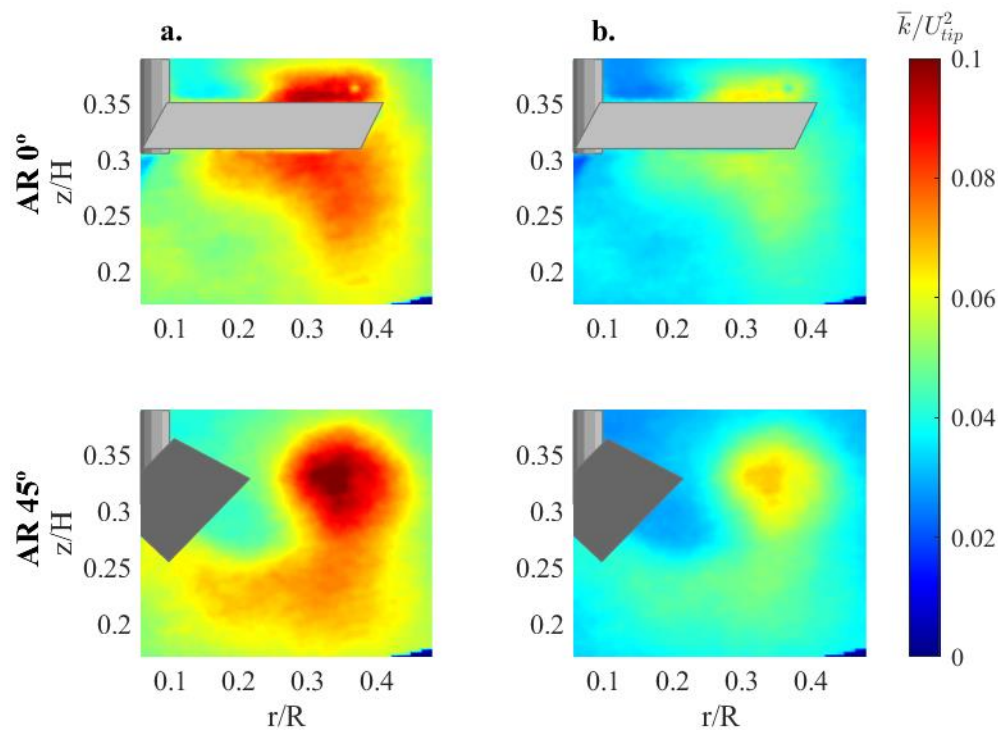


Fig. 5: Turbulent kinetic energy fields estimated by PIV-Camera 1 measurements considering (a) isotropic assumption and (b) only radial and axial velocity fluctuations at AR 0° and AR 45°.

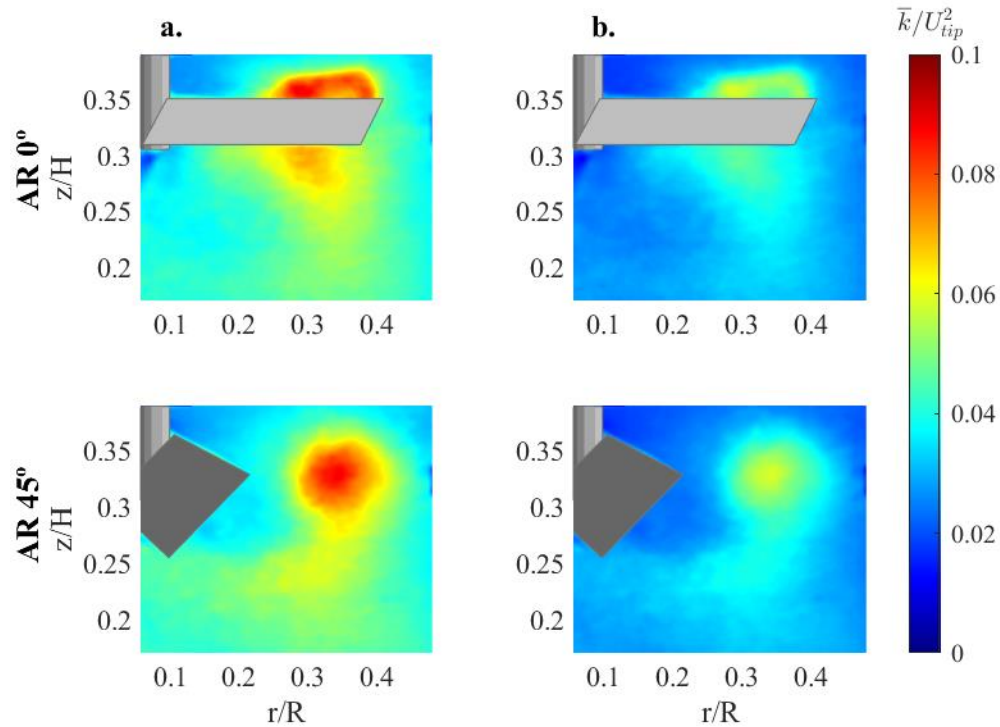


Fig. 6: Turbulent kinetic energy fields estimated by PIV-Camera 2 measurements considering (a) isotropic assumption and (b) only radial and axial velocity fluctuations at AR 0° and AR 45°.

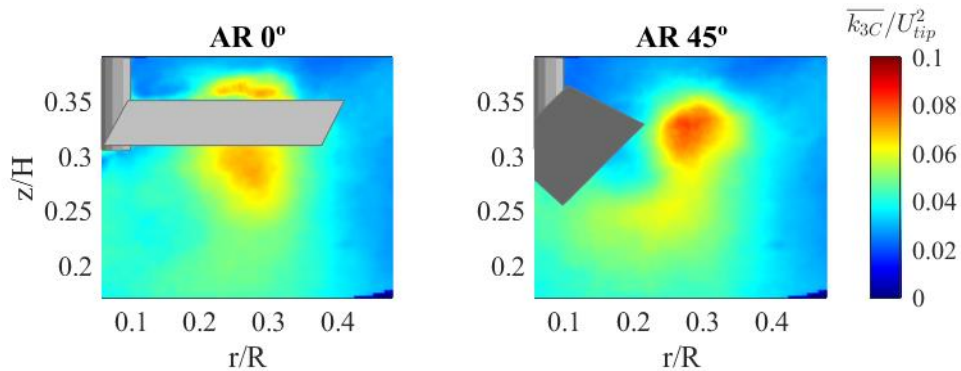


Fig. 7: Turbulent kinetic energy fields estimated by Stereo-PIV measurements considering all three velocity fluctuations at AR 0° and AR 45°.

4. Conclusion

In this work, three different PIV techniques (PIV-Camera 1, PIV-Camera 2 and Stereo-PIV) were applied to perform angle-resolved measurements in two different blade angle positions of 0° and 45°. Additionally, the turbulent kinetic energy estimation was computed considering three distinct approaches: the isotropic approximation, the non-isotropic assumption and the computation with all three velocity fluctuations. The results allowed to investigate the influence of these criteria (technique, blade angle and TKE estimation approach) on the analysis of the flow promoted by a pitched-blade turbine in a stirred tank. Regarding the flow pattern, it was verified that the radial component fields obtained by the PIV-Camera 1 have higher values than those obtained by the PIV-Camera 2 and Stereo-PIV. This can be associated with the perspective error due to the more tilted positioning of the camera so that the radial component has its values

overestimated and influenced by the tangential component (out-of-plane velocity). The flow presented a strongly downward axial pattern due to the movement induced by the down-pumping pitched-blade turbine and it was possible to observe the motion of the trailing vortices from the suction region at AR 0° to the discharge region at AR 45°, suffering a slight deviation due to the pitched blade.

The TKE fields for all the techniques showed that the turbulent kinetic energy is concentrated in the region of the trailing vortices formation, following its movement from the suction region (above the turbine), at AR 0°, to the discharge region (below the turbine), at AR 45°. For the PIV-Camera 1 technique, the pseudo-isotropic assumption tends to overestimate the TKE values as a consequence of the higher values obtained for the radial component. The TKE fields obtained by PIV-Camera 2 with non-isotropic approximation and by Stereo-PIV present similar results. This can suggest that the PIV-Camera 2 technique is a more suitable arrangement because it shows similar information comparing to the Stereo-PIV setup with a simpler and more economical system. The following steps of the work involve the analysis of these parameters in other flow patterns promoted by different impeller types as well as evaluating multiphase systems.

Acknowledgments

The authors would like to express their gratitude to Petrobras S/A (grant No. 2017/00376-1) and CNPq (grant No. 142604/2019-4 and No. 140997/2019-9) for the financial support provided. The authors would also like to thank the *PIVbr group* (www.piv.eng.br) for their collaboration and support on image processing.

References

- [1] S. Basu, "Multiphase Flow Measurement," in *Plant Flow Measurement and Control Handbook*, vol. 2, Elsevier, 2019, pp. 803–926.
- [2] H. Unadkat, C. D. Rielly, G. K. Hargrave, and Z. K. Nagy, "Application of fluorescent PIV and digital image analysis to measure turbulence properties of solid-liquid stirred suspensions," *Chem. Eng. Res. Des.*, vol. 87, no. 4, pp. 573–586, 2009, doi: 10.1016/j.cherd.2008.11.011.
- [3] M. Raffel, C. E. Willert, F. Scarano, C. J. Kähler, S. T. Wereley, and J. Kompenhans, *Particle Image Velocimetry*, 3rd ed. Cham: Springer International Publishing, 2018.
- [4] J. Westerweel, G. E. Elsinga, and R. J. Adrian, "Particle Image Velocimetry for Complex and Turbulent Flows," *Annu. Rev. Fluid Mech.*, vol. 45, no. 1, pp. 409–436, 2013, doi: 10.1146/annurev-fluid-120710-101204.
- [5] S. Kresta, "Turbulence in stirred tanks: anisotropic, approximate, and applied," *Can. J. Chem. Eng.*, vol. 76, no. 3, pp. 563–576, Jun. 1998, doi: 10.1002/cjce.5450760329.
- [6] A. K. Prasad, "Stereoscopic particle image velocimetry," *Exp. Fluids*, vol. 29, no. 2, pp. 103–116, Aug. 2000, doi: 10.1007/s003480000143.
- [7] A. D. Barbutti, A. G. De Mitri, J. S. Ayala, R. de L. Amaral, H. L. de Moura, J. R. Nunhez, G. J. de Castilho, "Compensation of Image Distortion on PIV Measurements of a Stirred Tank," in *12th Spring School on Transition and Turbulence*, 2020, doi: 10.26678/ABCM.EPTT2020.EPT20-0101.
- [8] S. M. Soloff, R. J. Adrian, and Z. C. Liu, "Distortion compensation for generalized stereoscopic particle image velocimetry," *Meas. Sci. Technol.*, vol. 8, no. 12, pp. 1441–1454, 1997, doi: 10.1088/0957-0233/8/12/008.
- [9] B. J. Kim and H. J. Sung, "A further assessment of interpolation schemes for window deformation in PIV," *Exp. Fluids*, vol. 41, no. 3, pp. 499–511, 2006, doi: 10.1007/s00348-006-0177-y.
- [10] F. Scarano, "Iterative image deformation methods in PIV," *Meas. Sci. Technol.*, vol. 13, no. 13, pp. 1–19, 2002, Accessed: Jul. 16, 2020. [Online]. Available: www.pivchallenge.org.
- [11] A. Eckstein and P. P. Vlachos, "Digital particle image velocimetry (DPIV) robust phase correlation," *Meas. Sci. Technol.*, vol. 20, no. 5, 2009, doi: 10.1088/0957-0233/20/5/055401.
- [12] J. Westerweel and F. Scarano, "Universal outlier detection for PIV data," *Exp. Fluids*, vol. 39, no. 6, pp. 1096–1100, 2005, doi: 10.1007/s00348-005-0016-6.
- [13] A. D. Barbutti, R. de L. Amaral, H. L. de Moura, F. de A. Oliveira Júnior, J. R. Nunhez, and G. J. de Castilho, "A New Field Correction Method For Piv Measurements Based On Mutual Information: Case Study On A Stirred Tank Flow," *Measurement*, vol. 186, no. August, p. 110130, 2021, doi: 10.1016/j.measurement.2021.110130.
- [14] F. R. Khan, C. D. Rielly, and D. A. R. Brown, "Angle-resolved stereo-PIV measurements close to a down-pumping

pitched-blade turbine,” *Chem. Eng. Sci.*, vol. 61, no. 9, pp. 2799–2806, 2006, doi: 10.1016/j.ces.2005.10.067.